Proposal of novel ultra-violet lasers using BeZnMgSe heterostructure lattice matched to silicon

Takeo MARUYAMA, Naoto NAKAMURA, Yuki NIIYAMA and Masahiro WATANABE

Department of Information Processing, Tokyo Institute of Technology
4259 Nagatsuta-cho, Midori-ku, Yokohama 226-8502, Japan
E-mail: maruyama@pe.titech.ac.jp

We propose a II-VI semiconductor laser using BeMgZnSe which lattice matched to Si. The threshold current density of the laser is calculated using the density-matrix theory. The threshold current density under 1kA/cm^2 is estimated for a single QW laser structure. BeZnSe alloys have been grown by MBE on CaF_2/Si(111) and GaP(001) substrate. The crystalline quality and surface morphology are different by buffer layers because of the surface energy of these layers. The atomically flat BeZnSe layer is obtained on GaP(001). PL from UV region is observed at band edge at 17K.

1. Introduction

The interest in wide band gap II-VI semiconductors has been intense during the past decade because of their possible applications in short wavelength optoelectronic devices. Among them, Be-chalcogenides are considered to be promising materials for devices operating in the blue-UV spectral region (Fig.1). The atomic bonding in Be-compound has a more covalent character than others II-VI semiconductors such as ZnSe.[1] This leads to an increase of the stacking faults energies in these materials, which is expected to improve the degradation behavior of the devices based on Be-compounds.

In the case of BeMgZnSe alloys, a wide range of band-gap energies is covered by varying the composition and furthermore these compounds can be lattice matched on Si substrate. Therefore these compounds are an attractive material towards opto-electronic integrated circuit.

Crystal growth of BeZnSe on Si substrate has already been demonstrated. However this growth is plagued with many difficulties, in particular that of a Si-Se chemical reaction, which are not completely overcome at this stage.

In this letter, we report on the proposal and theoretical estimation of the threshold current density of quantum well (QW) laser using BeZnMgSe, and the epitaxy of ZnBeSe onto CaF_2/Si(111), GaP(001) substrate to check the availability using the buffer layer to avoid the chemical reaction at the interface.

2. Proposal and analysis of BeMgZnSe QW laser

Figure 2 shows the analysis model of the laser structure proposed in this study. The model is constructed by the separated confinement

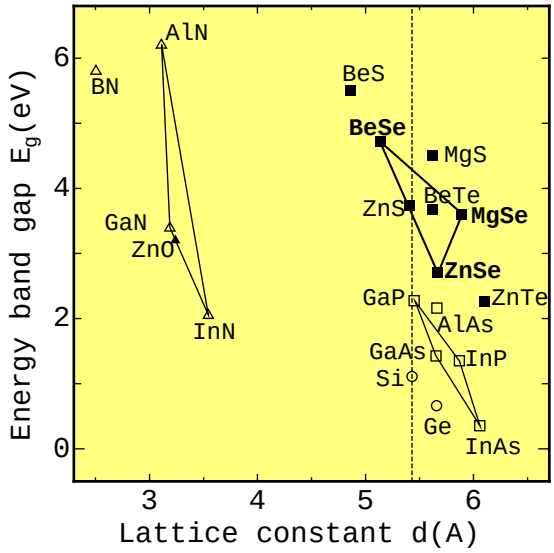

Fig.1: Relation between the energy band gap and the lattice constant. Broken line shows the lattice constant of Si substrate.

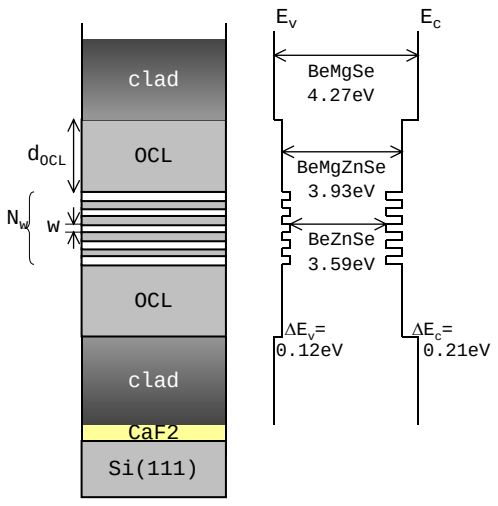

Fig.2: Schematic diagram of the bandgap structure of the BeZnSe/BeMgZnSe/BeMgSe QW laser.

heterostructures (SCH). We have known only the lattice constants and the energy band gaps of BeSe, MgSe and ZnSe. Other material parameters, effective mass and band offset, were estimated from relations between band gap and material parameters of conventional III-V and II-V compound semiconductors. Oscillation energy and dispersion energy, which are used to calculate the refractive index from MSEO method, were also estimated in the same way.

The laser gain g and radiative carrier lifetime τ_r are calculated by use of the density-matrix method,[3,4] well established for III-V semiconductor lasers.

The threshold gain g_{th} for lasing is expressed by

$$g_{th} = \alpha_{ac} + (1-\xi)\alpha_{ex}/\xi + \ln(1/R)/(\xi L)$$

where α_{ac} and α_{ex} are the optical loss in the active layer and the other layers, respectively, L the cavity length, R the end mirror reflectivity, and ξ the optical confinement factor in the active region. The ξ value is obtained by electromagnetic analysis using the refractive indices of the laser waveguide layers. R can be estimated from $R = (n\text{-}1)^2/(n+1)^2$. α and L are assumed to be $10cm^{-1}$ and 300μm, respectively.

The threshold current density can be estimated from

$$J_{th} = ewN_w N_{th}/\tau_r$$

where e, w, N_w and N_{th} are electronic charge, quantum well width, number of quantum wells and threshold carrier density, respectively. In this calculation, the nonradiative recombination lifetime was neglected because the Auger recombination of the major factor in nonradiative recombination is small at wide band gap materials.[5]

The calculated threshold current density is shown as a function of the number of wells and well width in Fig. 3. The threshold current density value of under below $1kA/cm^2$ was theoretically calculated in a single QW of thinner than 7nm in width.

3. Crystal growth of BeZnSe

Epitaxial growth of BeZnSe on Si substrate was reported using As adsorption layer to avoid the Se-Si reaction which leads to the formation of an amorphous compound at the interface. However this film was not so good crystalline quality because the reaction is not prevented completely.[1]

CaF_2, GaP and ZnSe are good candidate for buffer layers because these materials have lattice constant close to that of Si. Among them, we

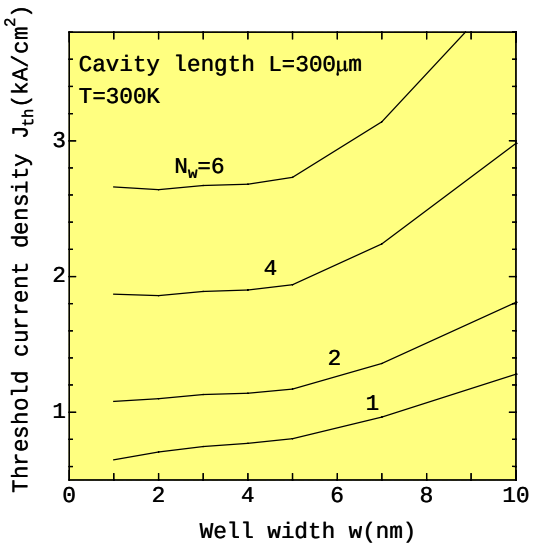

Fig.3: Theoretical threshold current densities of the BeZnSe/BeMgZnSe/BeMgSe QW lasers as a function of a QW width and a number of the QW.

chose CaF_2 and GaP because these can be grown using MBE technique.

An ultra-high vacuum (UHV) molecular beam epitaxy (MBE) system (background pressure ~ 10^{-9} Torr) was used in this study. The system was equipped with five effusion cells for Be, Mg, Zn, Se and CaF_2. CaF_2 molecular beams can be ionized by electron bombardment, which enhances the migration energy of CaF_2. The MBE system was also equipped with RHEED for surface structural studies. The as-grown samples were characterized by high-resolution x-ray diffraction (XRD) measurements. For spectroscopic studies, the He cryostat maintained at 17K. photoluminescence (PL) was excited by the 193nm line of pulsed ArF excimer laser.

3-1. Crystal growth on CaF_2/Si(111)

An n-type Si(111) substrate was chemically cleaned and a protective oxide layer was formed.

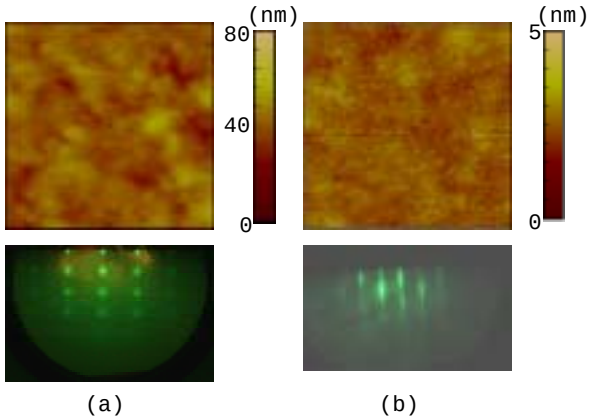

Fig. 4: AFM image and RHEED pattern of BeZnSe layer grown on (a) CaF_2/Si(111) substrate and (b) GaP(001) substrate.

After the substrate was loaded into the UHV chamber, the oxide was removed at 900°C, which resulted in an atomically clean Si surface with 7×7 reconstruction. A 10 nm-thick CaF_2 layer was epitaxially grown on the Si substrate at deposition rate of 0.3nm/min at substrate temperature of 700°C with 2-3% ionized CaF_2 flux during the initial stage of growth. This yielded a atomically flat CaF_2(111) epilayer with a maximum roughness of less than 1nm. After the growth of CaF_2, BeZnSe was grown at growth temperature range of 150°C–250°C, thickness of 200nm and growth rate of 2nm/min. The RHEED pattern of BeZnSe indicated halo, ring and spotty at 150°C, 190°C and 250°C, respectively. To obtain the single crystalline quality, growth temperature of higher than 250°C is required.

3-2. Crystal growth on GaP(001)

An n-type GaP(001) substrate was chemically cleaned. The in-situ desorption of the oxide was performed by heating the substrate at 500°C. We have investigated the crystalline quality and the flatness of the GaP substrate by RHEED and atomic force microscopy (AFM), respectively. The root mean square (rms) roughness has been measured to be 0.5nm for 1μm scan.

BeZnSe was grown at growth temperature of 250°C, thickness of 100nm, growth rate of 0.1μm/h and II/VI ratio of VI-rich. RHEED pattern and AFM image of as-grown sample is shown Fig. 4(b). The atomically flat BeZnSe was achieved at this condition.

4. Influence of buffer layer

BeZnSe on Si substrate always nucleates via a 3D growth mode but even under lattice-matching condition. Contrary to the case of the epitaxy onto Si, BeZnSe on GaP substrate was grown with flat surface. (Fig. 4)

The result was caused by the difference of surface morphology. The surface energy of base material and epi material is indicated as γ_{base} and γ_{epi}, respectively. It is known that if $\gamma_{base} > \gamma_{epi}$, the film is grown by step flow mode and if $\gamma_{base} < \gamma_{epi}$, the film is grown by island growth mode.

Table 1 shows the surface energy of CaF_2 and GaP. γ of CaF_2(111) is minimum value and γ of GaP(001) is maximum value in this table. γ of conventional semiconductors are rage of 1-2. Therefore, GaP is more suitable for buffer layer from the viewpoint of the surface morphology.

Table 1: Surface energy of CaF_2 and GaP.

	γ(J/m^2)		
	(001)	(011)	(111)
CaF_2	1.51	0.94	**0.47**
GaP	**2.9**	2.0	1.7

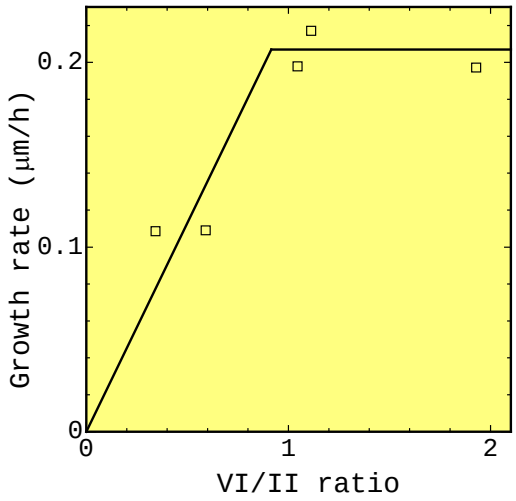

Fig.5: VI/II flux ratio dependence of growth rate of BeZnSe at 250°C.

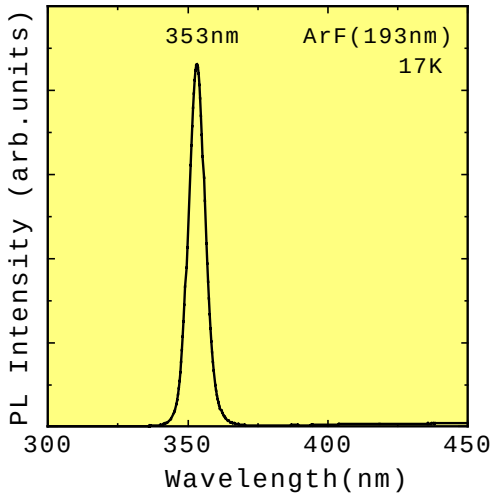

Fig.6: PL spectrum of BeZnSe on GaP at 17K.

5. Crystal growth condition dependence of BeZnSe quality

Growth condition dependences of BeZnSe (II/VI flux ratio dependence of growth rate, Be content dependence of PL) have been demonstrated grown on GaP substrate. The growth rate of the film depends both on the flux and on the substrate temperature. Figure 5 shows the measured growth rate of BeZnSe at 250°C as a function of VI/II ratio. The growth rate increases almost in proportion to VI/II ratio when VI/II <1, and growth rate tends to saturate when VI/II > 1. When VI/II = 1, the crystalline quality and surface morphology are most good.

A PL spectrum of BeZnSe on GaP substrate at

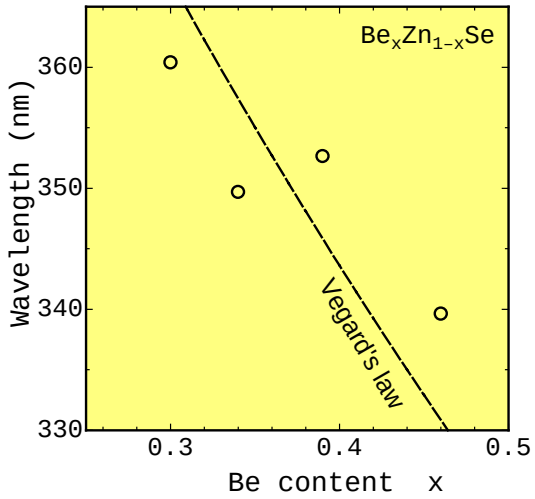

Fig.7: Be content dependence of PL wavelength.

17K is shown Fig.6. The PL emission of BeZnSe was observed at UV region from band edge. Figure 7 shows the Be content dependence of PL wavelength. The wavelength is matched to Vegard's law.

6. Conclusion

We proposed a II-VI semiconductor laser using BeMgZnS which lattice matched to Si. We estimated the threshold current density of the laser using the density-matrix theory. The value of threshold current density was calculated under 1kA/cm^2 in a single QW of thinner 7nm in width. BeZnSe alloys have been grown by MBE on CaF_2/Si(111) and GaP(001) substrate. The atomically flat surface of BeZnSe was obtained at GaP(001) surface. PL from UV region of band edge was observed at 17K.

References

1) F. Ficher, G. Landwehr, Th. Litz, H.J. Lugauer, U. Zehnder, Th. Gerhard, W. Ossau and A. Waag: *J. Cryst. Growth*, **175/176**, pp.532-540, 1997.
2) J.P. Faurie, V. Bousquet, P. Brunet and E. Tournie: *J. Cryst. Growth*, **184/185**, pp.11-15, 1998.
3) M. Asada, A. Kameyama and Y. Suematsu: *IEEE J. Quantum Electron.*, **QE-20**, pp. 745-752, 1984.
4) M. Yamada and H. Ishiguro: *Jpn. J. Appl. Phys.*, **20**, pp. 1279-1288, 1981.
5) A. Sugimura: IEEE J. Quantum Electron., QE18, pp. 352-355 1982